

ARTICLE

Supporting Information

Versatile and Cost-efficient Cleanup of Viscous Crude Oil by Elastic Carbon Sorbent from Direct Pyrolysis of Melamine Foam

Haifeng Niu,^a Jianbo Li,^{*a} Zhe Qiang^{*b} and Jie Ren^{*a}

^a Institute of Nano and Biopolymeric Materials, Department of Polymeric Materials, Key Laboratory of Advanced Civil Engineering Materials (Ministry of Education), School of Materials Science and Engineering, Tongji University, 4800 Caoan Road, Shanghai 201804, China.

^b School of Polymer Science and Engineering, University of Southern Mississippi, Hattiesburg, MS, USA, 39406

E-mail: Jianbo Li (Email: lijianbo@tongji.edu.cn), Zhe Qiang (Email: zhe.qiang@usm.edu); Jie Ren (Email: renjie6598@163.com)

Table of Content

Figure S1. SEM images of the CMF sponge.

Figure S2. Compressive mechanical behavior of CMF.

Figure S3. Compressive mechanical behavior of MF.

Figure S4. Organic solvents/oil absorption capacities.

Figure S5. Oil-water separation performance of CMF.

Figure S6. Combustion of ethanol absorbed in CMF.

Figure S7. Wetting behaviour of crude oil on CMF surface at room temperature.

Figure S8. Infrared thermal imaging of CMF under 0.5 sunlight.

Figure S9. Temperature evolution of CMF as a function time under different conditions.

Figure S10. Comparison of the final temperature of different sorbents after solar- or Joule-heating.

Figure S11. The changes of the absorption capacity of CMF under different conditions.

Figure S12. The recovery process of crude oil under solar- or Joule-heating.

Table S1. Element content of MF and CMF obtained by XPS.

Table S2. Absorption performance for crude oil recovery and the water contact angle of sorbent from our work and other previous reports.

Video S1: the CMF exhibits excellent elasticity and can be fully recovered to its original state without any visible damage or fracture after being deformed by various means, including bending, twisting and curling.

Video S2: Combustion of ethanol absorbed in CMF.

Video S3: The recovery process of crude oil under solar- and Joule-heating recorded by a camera.

Video S4: The recovery process of crude oil under solar- and Joule-heating recorded by the infrared camera.

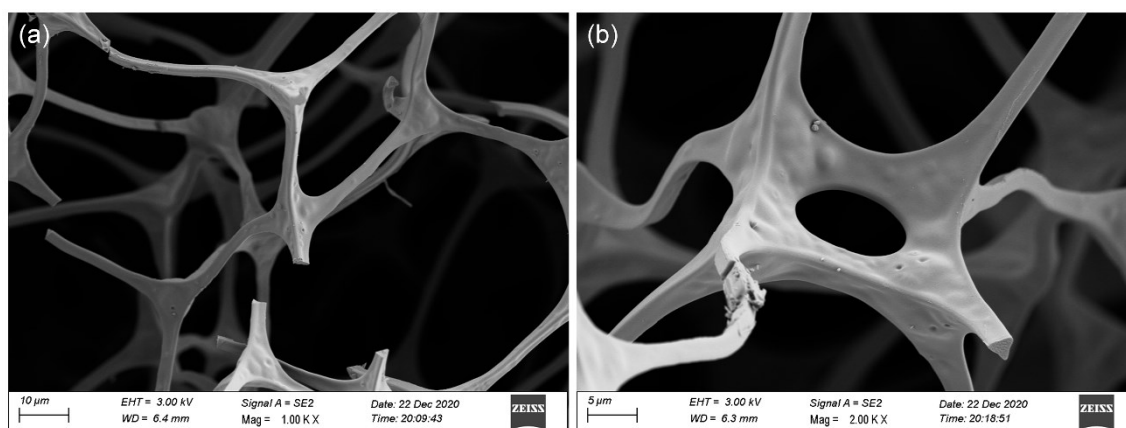


Figure S1. SEM images of the CMF sponge to show scaffold surface roughness.

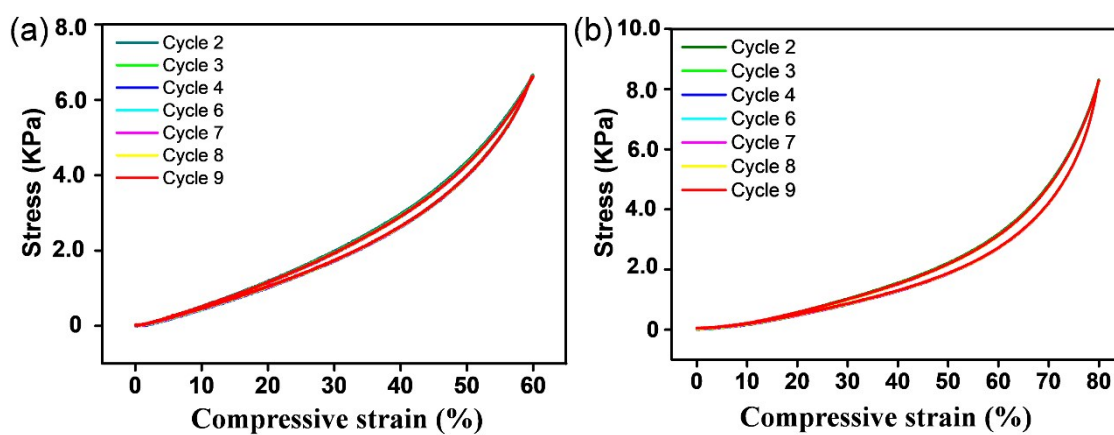


Figure S2. Compressive mechanical behavior of CMF at deformation rate of 5 mm/min with a maximum strain of (a) 60% and (b) 80%.

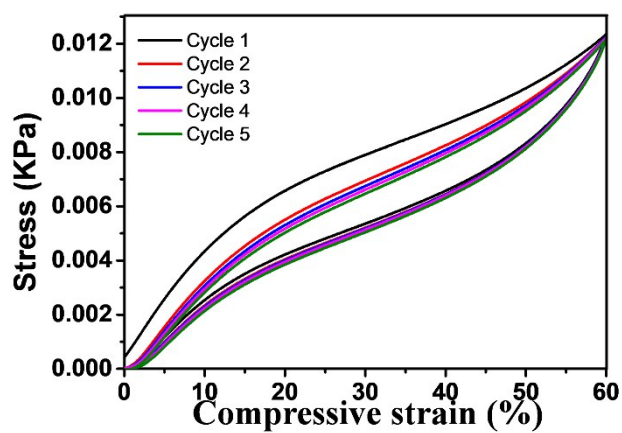


Figure S3. Compressive mechanical behavior of MF at deformation rate of 5 mm/min with a maximum strain of 60%.

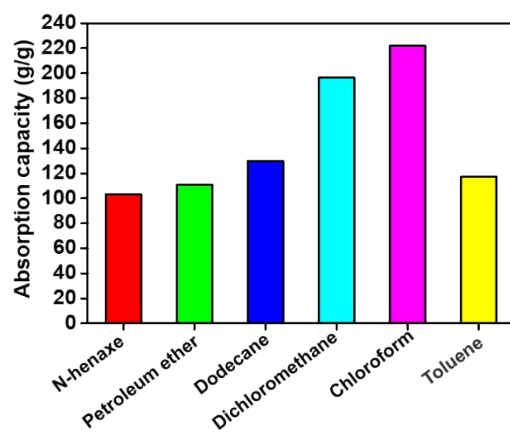


Figure S4. Organic solvents/oil absorption capacities of CMF.

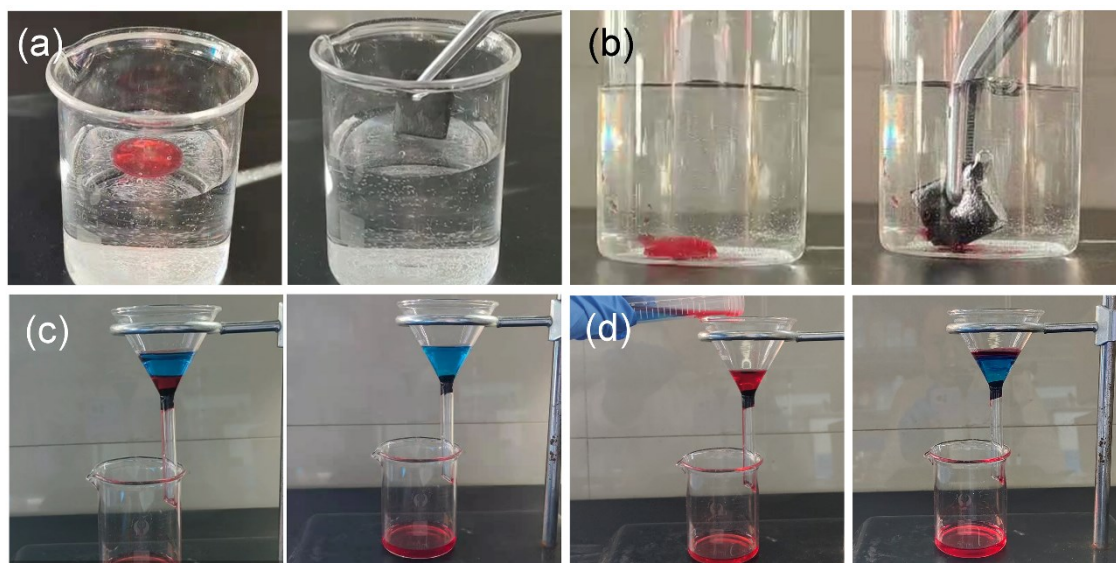


Figure S5. Pictures of CMF sponge for absorbing different oils (dyed with Oil Red O), (a) toluene (lighter than water), (b) chloroform (heavier than water). Pictures of CMF sponge for separating different oils (dyed with Oil Red O), (c) toluene (lighter than water), (d) chloroform (heavier than water).

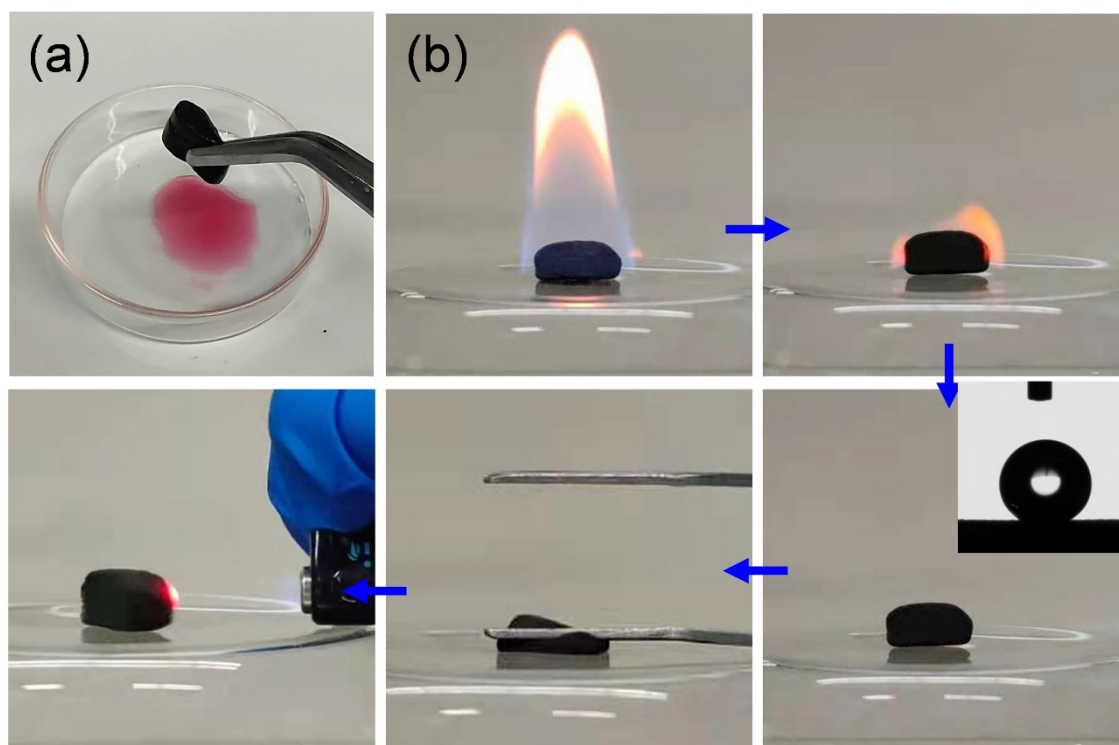


Figure S6. (a) Squeezing n-hexane (Oil red O) from CMF sponge. (b) Combustion of ethanol absorbed in CMF sponge. The water contact angle remains unchanged after a combustion process.

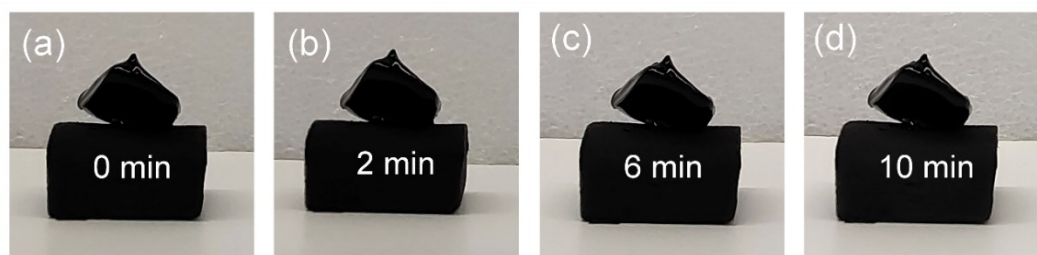


Figure S7. Wetting behavior of crude oil on CMF surface at room temperature after 10 min.

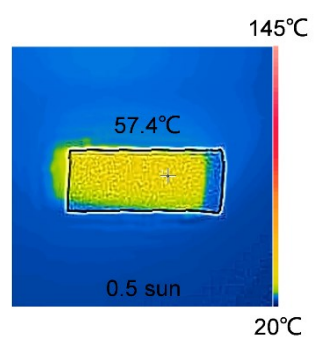


Figure S8. Infrared thermal imaging of CMF under 0.5 sunlight.

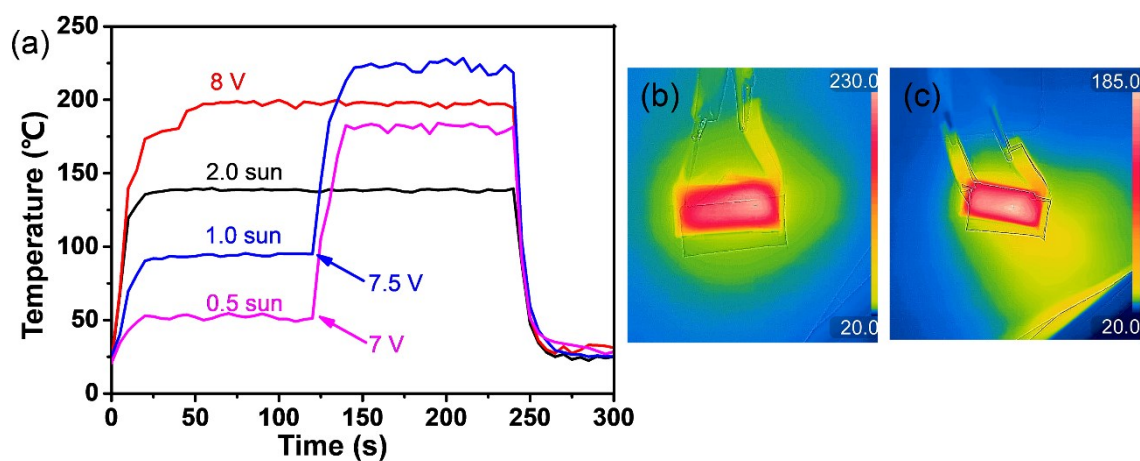


Figure S9. (a) Temperature evolution of CMF (3.1 cm × 1.6 cm × 0.8 cm) as a function time under different conditions. (b) Under 1.0 sunlight irradiation, the infrared images of the CMF with voltage of 7.5 V. (c) Under 0.5 sunlight irradiation, the Infrared images of the CMF with voltage of 7 V.

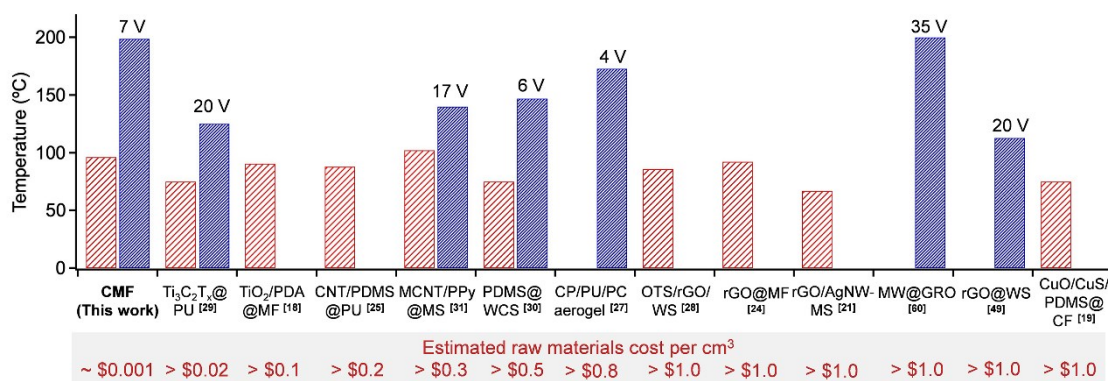


Figure S10. Comparison of the final temperature of different sorbents after solar- or Joule-heating. For all solar heating temperatures (left column in red), the intensity for the experiments is 1.0 sunlight. For all Joule heating temperatures (right column in blue), the applied voltage was all labelled. We also provided the estimated unit cost of raw materials for fabricating different sorbents on the bottom. While these prices could change upon the selection of vendors, CMF is apparently much cheaper than others since it only requires a step of direct carbonization of MF.

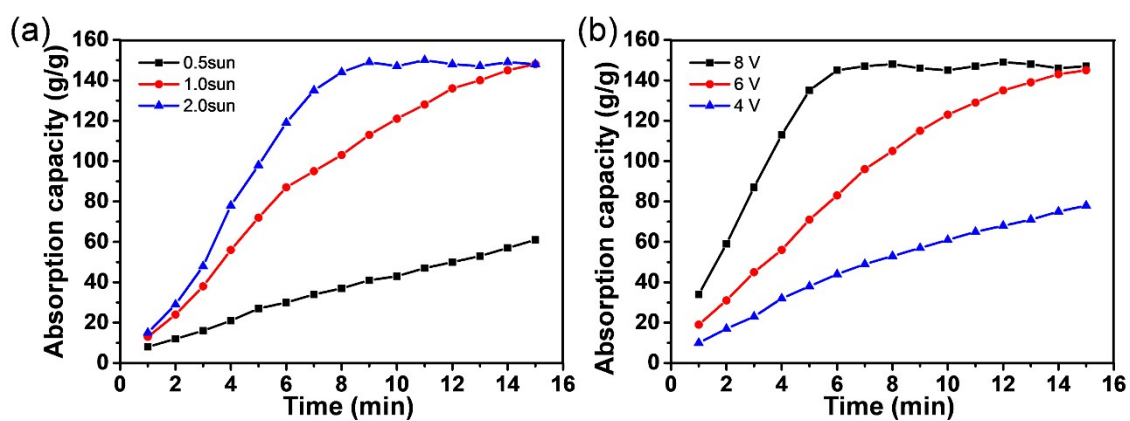


Figure S11. (a) The changes of the absorption capacity of CMF (3.1 cm × 1.6 cm × 0.8 cm) with time under different light intensities (no voltage), (b) The changes of the absorption capacity of CMF (3.1 cm × 1.6 cm × 0.8 cm) with time at different voltages (without light).

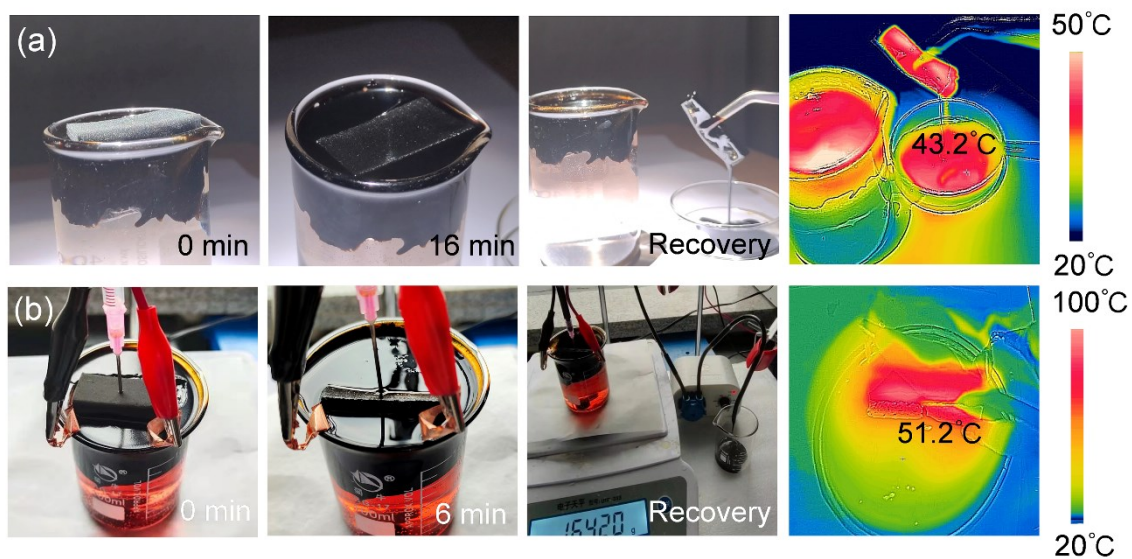


Figure S12. (a) The photograph of recovery process of crude oil using a piece of CMF sponge (3.1 cm \times 1.6 cm \times 0.5 cm) under sunlight irradiance (1.0 sunlight). (b) The photograph of recovery process of crude oil using a piece of CMF sponge (3.1 cm \times 1.6 cm \times 0.8 cm) with applied voltage of 8 V.

Table S1. Element content of CMF obtained by XPS.

	CMF (at%)	MF (at%)
C 1s	84.1%	67.61%
N 1s	2.78%	10.4%
O 1s	12.07%	21.99%

Table S2. Absorption performance for crude oil recovery and the water contact angle of sorbent from our work and other previous reports.

Sorbents	WCA	Absorption capacity (Crude oil)	Reference
CuO@CuS/PDMS NWAs/CF sponge	151±0.6°	1.3 g cm ⁻³	1
CNT/PDMS-PU sponge	154°± 0.8°	17.5 g g ⁻¹	2
Ti ₃ C ₂ TX@PU	122°	48 g g ⁻¹	3
PDMS@WCS	154°	0.80 g cm ⁻³	4
m-CNT/PPy@MS	158°	83.3 g g ⁻¹	5
F-rGO@WS wood sponge	145°	4.63 g g ⁻¹	6
MW@RGO	131°	N/A	7
CP/PU/PC aerogel	135°	N/A	8
CMF	151±2°	148.7 g g ⁻¹ or 0.8 g cm ⁻³	This work

Video S1. The CMF exhibits excellent elasticity and can be fully recovered to its original state without any visible damage or fracture after being deformed by various means, including bending, twisting and curling. Video have been sped up by 3x.

Video S2. Combustion of ethanol absorbed in CMF, there is no obvious change in the elasticity of the sponge after combustion. Video have been sped up by 3x.

Video S3. The recovery process of crude oil under solar- and Joule-heating recorded by a camera. Video have been sped up by 3x.

Video S4. The recovery process of crude oil under solar- and Joule-heating recorded by the infrared camera. Video have been sped up by 3x.

References

- 1 Q. Li, Q. Sun, Y. Li, T. Wu, S. Li, H. Zhang and F. Huang, *ACS Appl. Mater. interfaces*, 2020, **12**, 19476-19482.
- 2 J. Chang, Y. Shi, M. Wu, R. Li, L. Shi, Y. Jin, W. Qing, C. Tang and P. Wang, *J. Mater. Chem. A*, 2018, **6**, 9192-9199.
- 3 C. Gong, J. Lao, B. Wang, X. Li, G. Li, J. Gao, Y. Wan, X. Sun, R. Guo and J. Luo, *J. Mater. Chem. A*, 2020, **8**, 20162-20167.
- 4 M. B. Wu, S. Huang, T. Y. Liu, J. Wu, S. Agarwal, A. Greiner and Z. K. Xu, *Adv. Funct. Mater.*, 2020, **31**, 2006806.
- 5 X. Wu, Y. Lei, S. Li, J. Huang, L. Teng, Z. Chen and Y. Lai, *J. Hazard. Mater.*, 2021, **403**, 124090.
- 6 W. Huang, L. Zhang, X. Lai, H. Li and X. Zeng, *Chem. Eng. J.*, 2020, **386**, 123994.
- 7 J. Ge, L. A. Shi, Y. C. Wang, H. Y. Zhao, H. B. Yao, Y. B. Zhu, Y. Zhang, H. W. Zhu, H. A. Wu and S. H. Yu, *Nat. Nanotechnol.*, 2017, **12**, 434-440.
- 8 Y. Wang, L. Chen, H. Cheng, B. Wang, X. Feng, Z. Mao and X. Sui, *Chem. Eng. J.*, 2020, **402**, 126222.